

Large-scale magnetic fields, curvature fluctuations and the thermal history of the Universe

Massimo Giovannini ¹

Centro “Enrico Fermi”, Via Panisperna 89/A, 00184 Rome, Italy

Department of Physics, Theory Division, CERN, 1211 Geneva 23, Switzerland

Abstract

It is shown that gravitating magnetic fields affect the evolution of curvature perturbations in a way that is reminiscent of a pristine non-adiabatic pressure fluctuation. The gauge-invariant evolution of curvature perturbations is used to constrain the magnetic power spectrum. Depending on the essential features of the thermodynamic history of the Universe, the explicit derivation of the bound is modified. The theoretical uncertainty in the constraints on the magnetic energy spectrum is assessed by comparing the results obtained in the case of the conventional thermal history with the estimates stemming from less conventional (but phenomenologically allowed) post-inflationary evolutions.

arXiv:0707.0857v1 [astro-ph] 5 Jul 2007

¹e-mail address: massimo.giovannini@cern.ch

1 Introduction

It is tempting to speculate that large-scale magnetic fields are generated in the early Universe [1, 2, 3] during a phase where the Weyl invariance of their evolution equations is broken either spontaneously or explicitly (see, for instance, [4] and references therein). As a result the obtained magnetic fields will be necessarily tangled over typical wavelengths larger than the Hubble radius [5, 6, 7, 8, 9]. In this situation, the presence of magnetic fields may affect the evolution of curvature inhomogeneities in a way that is reminiscent of what happens in the presence of a non-adiabatic pressure fluctuations.

Suppose, indeed, that large-scale magnetic fields are generated thanks to the amplification of the quantum fluctuations of an Abelian gauge field which can be identified with the hypercharge field whose modes will not be screened by thermal effects. In spite of the specific model of parametric amplification, the result of the process will be a stochastically distributed field whose two point function can be written as

$$\langle B_i(\vec{k}, \tau) B^j(\vec{p}, \tau) \rangle = \frac{2\pi^2}{k^3} P_i^j(k) P_B(k) \delta^{(3)}(\vec{k} + \vec{p}), \quad (1.1)$$

where $P_B(k)$ is the magnetic power spectrum (which may change depending upon the specific way the Weyl invariance is broken) and $P_i^j(k) = (\delta_i^j - k_i k^j / k^2)$ is the traceless projector. In Eq. (1.1) the momenta appearing in the correlator are the comoving wave-numbers. The homogeneous component of this configuration vanishes and, as a result, the magnetic fields will not break spatial isotropy ² of the background geometry whose line element can be written, in the spatially flat case and in terms of the conformal time coordinate τ , as

$$ds^2 = a^2(\tau)[d\tau^2 - d\vec{x}^2]. \quad (1.2)$$

The typical wavelengths that set the initial conditions of the CMB anisotropies ³ are still larger than the Hubble radius (i.e. $k\tau < 1$) at recombination, taking place for an approximate redshift $z_{\text{rec}} \sim 1050$ when the visibility function is peaked. When $k\tau < 1$ the evolution equations of the perturbations of the spatial curvature will receive contributions from three independent sources. The adiabatic mode typically provides the first contribution arising from the quantum fluctuations of a (single) inflaton field. The second contribution may come from a collection of non-adiabatic modes that may be present either because the inflationary evolution is driven by more than one scalar degree of freedom, or because the primordial plasma contains a number of spectator fields which do not drive the evolution of the background but whose inhomogeneities contribute to the overall fluctuations of the spatial curvature. Finally, the third contribution to the evolution of curvature fluctuations can be attributed to gravitating magnetic fields. Up to now various studies addressed the interplay between large-scale magnetic fields and the scalar [12, 13, 14] (see also [15, 16]), vector [17, 18, 19] and tensor [19] modes of the geometry (see [20] and [21] for two recent reviews). As far as the scalar modes are concerned, it was assumed that large-scale magnetic fields are present prior to recombination (but after equality) and the resulting corrections to the Sachs-Wolfe plateau have been computed [12, 13]. The analysis has been also recently extended to cover the Doppler region, i.e. the first, second and third peaks of the temperature autocorrelations [14]. The main theme of the present paper will be

²If a background magnetic field exist, it must necessarily be oriented along a specific direction [10]. The effective spatial isotropy is broken and the angular power spectrum depends on the direction of the magnetic field. As a consequence a number of constraints, stemming directly from the breaking of spatial isotropy, can be derived [11].

³By this expression we mean the wavelengths that set the initial conditions of the lowest multipoles of the Boltzmann hierarchy.

to discuss possible (further) numerical constraints arising from the coupled evolution of large-scale magnetic fields and curvature perturbations. This analysis, when correctly performed, allows to assess the theoretical uncertainty of the computational scheme. In fact, the results obtained in the case of the conventional thermal history can be compared with the estimates stemming from less conventional (but phenomenologically allowed) post-inflationary evolutions.

In the most simplistic ⁴ scenario a conventional inflationary phase is followed, after a sudden reheating, by a radiation-dominated phase which is replaced, at equality by the standard matter-dominated phase. This evolutionary history allows to compute the curvature perturbations that are induced, for instance, by a single primordial adiabatic mode. It is also possible, in the same framework, to include the peculiar effect of large-scale magnetic fields whose inhomogeneities may indeed affect the curvature perturbations [12, 13, 15, 16]. The result of this calculation allows the estimate of the Sachs-Wolfe plateau and, ultimately, the estimate of the Doppler oscillations [14].

If the evolutionary history of the background geometry changes in its early phases, also the effect of large-scale magnetic fields on the induced curvature perturbations will be different. The evolution of magnetized curvature perturbations is sensitive, both, to the total barotropic index and to the total sound speed, i.e.

$$w_t(\tau) = \frac{p_t}{\rho_t}, \quad c_{st}^2(\tau) = \frac{p'_t}{\rho'_t}, \quad (1.3)$$

where the prime denotes a derivation with respect to τ and the subscript t reminds that the barotropic index and the sound speed are the ones pertaining to the *total* fluid.

If the rate of expansion changes in the early phases of the thermal history of the Universe (typically prior to big bang nucleosynthesis) also w_t and c_{st}^2 will be different and the curvature perturbations will have a slightly different evolution. This qualitative argument will now be corroborated by a detailed calculation and this is one of the themes of the present investigation. The problem then becomes to estimate the total curvature perturbation that will be sensitive both to the adiabatic and to the magnetized contributions.

The strategy adopted in the present investigation will then be to scrutinize different thermodynamic histories of the Universe and to compute, in each of these cases, the resulting curvature perturbations for wavelengths that are still larger than the Hubble radius after matter-radiation equality. It will be shown that possible variations in the evolution of the total barotropic index will modify the interplay between the adiabatic and the magnetized components of curvature perturbations. This procedure will also allow to determine the theoretical error caused by selecting the most simplistic thermal history in comparison with its non-minimal counterparts.

The plan of the present analysis will then be the following. In section 2 the essential theoretical

⁴Notice that the most simplistic scenario is also the one contemplated by the minimal paradigm compatible with the three data sets that are used to infer the values of the cosmological parameters, i.e. the Λ CDM paradigm. These three data include, in general terms, the large-scale structure observations, by the CMB observations and by the type Ia supernovae observations. Before plunging into the discussion, it is appropriate to comment on the choice of the cosmological parameters that will be employed throughout this section. The WMAP data [22, 23, 24, 25, 26] have been combined, so far, with various sets of data. These data sets include the 2dF Galaxy Redshift Survey [27], the combination of Boomerang and ACBAR data [28, 29], the combination of CBI and VSA data [30, 31]. Furthermore the WMAP 3-year data have been also combined with the Hubble Space Telescope Key Project (HSTKP) data [32] as well as with the Sloan Digital Sky Survey (SDSS) [33, 34] data. Finally, the WMAP 3-year data can be also usefully combined with the weak lensing data [35, 36] and with the observations of type Ia supernovae (in particular the data of the Supernova Legacy Survey (SNLS) [37] and the so-called Supernova "Gold Sample" (SNGS) [38, 39]).

tools will be introduced. A consistent gauge-invariant description will allow to follow, in one shot, the evolution of the curvature fluctuations and of the density contrasts on comoving orthogonal hypersurfaces. In section 3 different models for the evolution of the barotropic index will be scrutinized and motivated. The resulting (magnetized) curvature perturbations will be computed. In section 4 a set of bounds on the magnetic field intensity will be derived and compared. Section 5 contains the concluding remarks.

2 Evolution equations

The notations ubiquitously employed in the present script imply that the Friedmann-Lemaître equations in the spatially flat case (with line element given in Eq. (1.2)) are given by:

$$\mathcal{H}^2 = \frac{8\pi G}{3} a^2 \rho_t, \quad (2.1)$$

$$\mathcal{H}^2 - \mathcal{H}' = 4\pi G a^2 (\rho_t + p_t), \quad (2.2)$$

$$\rho_t' + 3\mathcal{H}(\rho_t + p_t) = 0, \quad (2.3)$$

where $\mathcal{H} = a'/a$ and the prime denotes, as in Eq. (1.3) a derivation with respect to τ . Notice that $\mathcal{H} = aH$ where $H = \dot{a}/a$ is the Hubble expansion rate and the dot denotes a derivation with respect to the cosmic time coordinate t (recall that the connection between t and τ is given by the differential relation $dt = a(\tau)d\tau$). By virtue of the connection between \mathcal{H} and H , a given wavelength is larger than the Hubble radius provided the corresponding comoving wave-number k satisfies the condition $k/(aH) \simeq k\tau < 1$. Equations (1.3) and (2.3) imply

$$c_{\text{st}}^2 = w_t - \frac{w_t'}{3\mathcal{H}(w_t + 1)} = w_t - \frac{1}{3} \frac{d \ln(w_t + 1)}{d \ln a}, \quad (2.4)$$

so that $c_{\text{st}}^2 = w_t$ iff the (total) barotropic index is constant in time. For the purposes of the present investigation it is practical to start with the evolution equations of the fluctuations of the geometry expressed in fully gauge-invariant terms. The Hamiltonian and momentum constraints can be written as

$$\nabla^2 \Psi - 3\mathcal{H}(\mathcal{H}\Phi + \Psi') = 4\pi G a^2 (\delta\rho_t + \delta\rho_B), \quad (2.5)$$

$$\nabla^2 (\mathcal{H}\Phi + \Psi') = -4\pi G a^2 (1 + w_t) \rho_t \theta_t, \quad \theta_t = \nabla^2 V_t, \quad (2.6)$$

where $\delta\rho_t$ is the total (and gauge-invariant) density contrast of the fluid sources and $\delta\rho_B(\tau, \vec{x}) = B^2(\vec{x})/(8\pi a^4)$. The fluctuations Φ and Ψ are the gauge-invariant Bardeen potentials [40, 41] that coincide with the longitudinal fluctuations of the metric in the conformally Newtonian gauge. In Eq. (2.6) θ_t is the three-divergence of the total peculiar velocity. At the right-hand side of Eq. (2.6) the three-divergence of the Poynting vector leads to a term going as $\vec{\nabla} \cdot [\vec{E} \times \vec{B}]/a^4$, where $\vec{E} \simeq \vec{J}/\sigma \simeq (\vec{\nabla} \times \vec{B})/\sigma$ is the Ohmic electric field. The conductivity σ is large during most of the thermodynamic history of the Universe, since it is proportional to the temperature when the temperature is much larger than the mass of the corresponding species. The contribution of the Ohmic Poynting vector will therefore be neglected in comparison with the other components of the magnetic energy-momentum tensor. Introducing the density contrast on comoving orthogonal hypersurfaces, i.e.

$$\epsilon_m(\tau, \vec{x}) = \frac{\delta\rho_t + \delta\rho_B}{\rho_t} - 3\mathcal{H}(1 + w_t)V_t, \quad (2.7)$$

the Hamiltonian constraint (2.5) takes the peculiar form

$$\nabla^2\Psi = 4\pi G a^2 \rho_t \epsilon_m, \quad (2.8)$$

which is (just formally) analog to the Poisson equation typical of the non-relativistic treatment of gravitational inhomogeneities. Another relevant pair of gauge-invariant quantities is represented by

$$\zeta = -\Psi - \frac{\mathcal{H}(\delta\rho_t + \delta\rho_B)}{\rho_t'}, \quad (2.9)$$

$$\mathcal{R} = -\Psi - \frac{\mathcal{H}(\mathcal{H}\Phi + \Psi')}{4\pi G a^2 \rho_t (w + 1)}. \quad (2.10)$$

The variable ζ [41, 42] defined in Eq. (2.9), if evaluated in the gauge where the spatial curvature is uniform, is proportional to the total density contrast (as it can be directly checked by using Eq. (2.3)). The variable \mathcal{R} [42, 43], defined in Eq. (2.10), if evaluated on comoving orthogonal hypersurfaces, coincides with the fluctuations of the spatial curvature. It is clear that the three gauge-invariant variables defined, respectively, in Eqs. (2.7), (2.9) and (2.10) are all related by the Hamiltonian constraint. Inserting Eq. (2.3) into Eq. (2.9) and taking into account Eqs. (2.8), (2.10) and (2.5) the Hamiltonian constraint can be expressed in one of the following two equivalent forms:

$$\zeta = \mathcal{R} + \frac{\nabla^2\Psi}{12\pi G a^2 \rho_t (1 + w_t)}, \quad (2.11)$$

$$\zeta = \mathcal{R} + \frac{\epsilon_m}{3(1 + w_t)}, \quad (2.12)$$

where Eq. (2.12) follows from Eq. (2.11) making use of the generalized Poisson equation (2.8). It is relevant to remark that when the wavelengths are larger than the Hubble radius, at a given epoch,

$$\zeta \simeq \mathcal{R} + \mathcal{O}\left(\frac{k^2}{a^2 H^2}\right), \quad \epsilon_m \simeq \mathcal{O}\left(\frac{k^2}{a^2 H^2}\right). \quad (2.13)$$

In spite of the physical differences between ζ , \mathcal{R} and ϵ_m the explicit solution of the whole system in terms of one of these variables allows to compute the others. From the fluctuation of the covariant conservation equation of the total plasma the following equation can be easily obtained

$$\delta\rho_t' + 3\mathcal{H}(\delta\rho_t + \delta p_t) - 3(p_t + \rho_t)\Psi' + (p_t + \rho_t)\theta_t = 0. \quad (2.14)$$

Using now Eq. (2.9) inside Eq. (2.14) a first-order differential equation for ζ emerges and it is given by:

$$\zeta' = -\frac{\mathcal{H}}{\rho_t(1 + w_t)}\delta p_{\text{nad}} + \frac{\mathcal{H}(3c_{\text{st}}^2 - 1)}{3\rho_t(1 + w_t)}\delta\rho_B - \frac{\theta_t}{3}. \quad (2.15)$$

The term δp_{nad} in Eq. (2.15) accounts for the non-adiabatic pressure inhomogeneities; the following decomposition of the total pressure fluctuation

$$\delta p_t = \left(\frac{\delta p_t}{\delta\rho_t}\right)_\zeta \delta\rho_t + \left(\frac{\delta p_t}{\delta\zeta}\right)_{\rho_t} \delta\zeta \equiv c_{\text{st}}^2 \delta\rho_t + \delta p_{\text{nad}}, \quad (2.16)$$

has been tacitly assumed in Eqs. (2.14) and (2.15). While the first (adiabatic) contribution gives the pressure fluctuation produced by the inhomogeneous density fluctuation when the specific entropy is constant (i.e. $\delta\zeta = 0$), the second (non-adiabatic) contribution arises even if the density is unperturbed (i.e. $\delta\rho_t = 0$) but the plasma possesses many different components (for instance, in the pre-recombination plasma, photons, baryons, neutrinos and dark matter).

The evolution of \mathcal{R} can be obtained, in similar terms, from the equations of Φ and Ψ , i.e.

$$\Psi'' + \mathcal{H}(\Phi' + 2\Psi') + (2\mathcal{H}' + \mathcal{H}^2)\Phi + \frac{1}{3}\nabla^2(\Phi - \Psi) = 4\pi G a^2(\delta p_t + \delta p_B), \quad (2.17)$$

$$\left(\partial_i \partial^j - \frac{1}{3}\delta_i^j \nabla^2\right)(\Phi - \Psi) = 8\pi G a^2(\Pi_i^j + \bar{\Pi}_i^j), \quad (2.18)$$

where Π_i^j is the anisotropic stress of the fluid and

$$\bar{\Pi}_i^j = \frac{1}{4\pi a^4} \left(B_i B^j - \frac{\delta_i^j}{3} B^2 \right) \quad (2.19)$$

is the anisotropic stress of the magnetic field. Inserting Eq. (2.10) into Eq. (2.17) and recalling Eq. (2.16) the evolution equation of \mathcal{R} can be written as

$$\mathcal{R}' = -\frac{\mathcal{H}}{\rho_t(1+w_t)}\delta p_{\text{nad}} + \frac{\mathcal{H}(3c_{\text{st}}^2 - 1)}{3\rho_t(1+w_t)}\delta\rho_B + \frac{\mathcal{H}}{12\pi G a^2(p_t + \rho_t)}\nabla^2(\Phi - \Psi) - \frac{\mathcal{H}c_{\text{st}}^2}{4\pi G a^2(p_t + \rho_t)}\nabla^2\Psi. \quad (2.20)$$

By now subtracting Eq. (2.20) from Eq. (2.15) and by using Eqs. (2.12) and (2.13), the appropriate equation of ϵ_m can be obtained after simple algebra:

$$\epsilon_m' - 3\mathcal{H}w_t\epsilon_m = -(1+w_t)\theta_t - 3\mathcal{H}(1+w_t)\Pi_t \quad (2.21)$$

where the notation

$$\partial_i \partial^j \Pi_j^i + \partial_i \partial^j \bar{\Pi}_j^i = (p_t + \rho_t)\nabla^2\Pi_t, \quad (2.22)$$

has been used. If there are collisionless particles in the plasma (like neutrinos, after weak interactions have fallen out of thermal equilibrium) we will have that

$$(p_t + \rho_t)\nabla^2\Pi_t = (p_\nu + \rho_\nu)\nabla^2\Pi_\nu + (p_\gamma + \rho_\gamma)\nabla^2\Pi_B. \quad (2.23)$$

Concerning Eq. (2.23) two comments are in order. We referred the magnetic anisotropic stress to the photon background. This is natural since, for typical length-scales larger than the magnetic diffusivity scale, both quantities redshift at the same rate with the expansion of the Universe. The second comment involves the relevance of the anisotropic stress. As discussed in relation with the estimate of the CMB autocorrelation induced by magnetic fields, the magnetic anisotropic stress is of utmost importance at intermediate scales. In particular the interplay with the neutrino anisotropic stress leads to the correct initial conditions for the magnetized CMB anisotropies. However, in the present paper we will be mostly concerned with the largest scales and we will try to assess what could be the influence, on those scales, of slightly different thermal histories of the Universe. For typical wavelengths larger than the Hubble radius at recombination the anisotropic stress can be neglected in the first approximation. If needed, however, it can be included with the standard iterative procedure [44, 45] (see also [46]) where, to lowest order, the solution is the one where $\Phi \simeq \Psi$.

3 Different thermal histories

By looking at Eq. (2.15) it is clear that, to leading order in $k^2\tau^2$, the evolution of ζ (and of \mathcal{R}) is determined by three independent pieces of information:

- the presence (or absence) of non-adiabatic pressure fluctuations;

- presence (or absence) of large-scale magnetic fields;
- the specific time dependence of w_t and c_{st}^2

The simplest possible situation compatible with the presence of super-Hubble magnetic fields arises when the Universe becomes suddenly dominated by radiation at the end of inflation. This is, incidentally, also the underlying assumption in the standard Λ CDM scenario. The Universe will then become dominated by dusty matter at a redshift⁵ $z_{\text{eq}} \simeq 3200$. If inflation was driven by a single inflaton and if other spectator fields with scale-invariant spectrum were absent, then it is also rather plausible to enforce the condition $\delta p_{\text{nad}} = 0$. In this situation, the exact solution of Eqs. (2.1), (2.2) and (2.3) implies that

$$w_t(\alpha) = \frac{1}{3(\alpha + 1)}, \quad c_{\text{st}}^2(\alpha) = \frac{4}{3(3\alpha + 4)}, \quad (3.1)$$

where

$$\begin{aligned} \alpha(\tau) &= \frac{a}{a_{\text{eq}}} = x^2 + 2x, & x &= \frac{\tau}{\tau_1}, \frac{a_0}{a_{\text{eq}}} = \frac{h_0^2 \Omega_{\text{M}0}}{h_0^2 \Omega_{\text{R}0}}, \\ \frac{a_0}{a_{\text{eq}}} &= \frac{h_0^2 \Omega_{\text{M}0}}{h_0^2 \Omega_{\text{R}0}}, & \tau_{\text{eq}} &= (\sqrt{2} - 1)\tau_{\text{eq}}. \end{aligned} \quad (3.2)$$

Using Eqs. (3.1) and (3.2) inside Eq. (2.15) and changing the variable from τ to α the following expression can be obtained:

$$\frac{d\zeta}{d\alpha} = -\frac{3R_\gamma \Omega_{\text{B}}}{(3\alpha + 4)^2}, \quad R_\gamma = \frac{\rho_\gamma(\tau)}{\rho_{\text{R}}(\tau)} \quad \Omega_{\text{B}}(\tau, \vec{x}) = \frac{\delta \rho_{\text{B}}(\tau, \vec{x})}{\rho_\gamma(\tau)}. \quad (3.3)$$

In Eq. (3.3) the magnetic energy density has been expressed in units of the photon energy density and R_γ denotes the photon fraction in the post-inflationary radiation background. After neutrinos decouple for temperatures of the order of the MeV the photon fraction will be related with the neutrino fraction as $R_\gamma = 1 - R_\nu$ where $R_\nu = 0.405$ (for three neutrino families). Direct integration of Eq. (3.3) gives the sought result, namely

$$\zeta(k, \tau) = \zeta_*(k) - \frac{3R_\gamma \Omega_{\text{B}(k)} \alpha(\tau)}{4(3\alpha(\tau) + 4)}. \quad (3.4)$$

The constant $\zeta_*(k)$ stands for the adiabatic mode produced (for instance during a phase of conventional inflation). After matter-radiation equality (but before recombination) to leading order in $k^2 \tau^2$ we will have, from Eq. (2.11), that

$$\mathcal{R}(k, \tau_{\text{rec}}) \simeq \zeta_*(k) - \frac{R_\gamma \Omega_{\text{B}}(k)}{4} \left(\frac{3\alpha_{\text{rec}}}{3\alpha_{\text{rec}} + 4} \right) + \mathcal{O}(k^2 \tau_{\text{rec}}^2), \quad \alpha_{\text{rec}} \simeq \frac{z_{\text{eq}} + 1}{z_{\text{rec}} + 1} = 3.07 \left(\frac{h_0^2 \Omega_{\text{M}0}}{0.134} \right). \quad (3.5)$$

This result can be easily interpreted from the physical point of view. When the rate of expansion increases from radiation to matter the barotropic index (and the sound speed) are both decreasing from 1/3 to 0. Thus the overall effect on the source term for the evolution of curvature perturbations implies that the magnetic contribution tends to cancel the contribution of the adiabatic mode.

⁵When not otherwise stated it will be assumed that $h_0^2 \Omega_{\text{M}0} \simeq 0.1326$, where $\Omega_{\text{M}0}$ denotes the present fraction in dusty matter. This value for the total critical fraction of matter emerges, in the context of the Λ CDM paradigm, when the WMAP data [22, 23] are combined with all the remaining cosmological data sets of different origin (excluding weak lensing data).

In the context of this reference scenario when the Universe only passes, after inflation, from radiation to matter also ϵ_m and θ_t can be computed, respectively, from Eqs. (2.8) and (2.6). It suffices to extract Ψ from ζ and then use the aforementioned constraints. Going to Fourier space result of this manipulation will be

$$\epsilon_m(k, \tau) = \frac{k^2 \tau_1^2}{12\alpha\sqrt{\alpha+1}} \left[\zeta_*(k) \mathcal{W}_1(\alpha) - \frac{3}{4} R_\gamma \Omega_B(k) \mathcal{W}_2(\alpha) \right], \quad (3.6)$$

$$\theta_t(k, \tau) = -\frac{k^2 \tau_1}{2} \left\{ \left[\frac{\alpha}{\sqrt{\alpha+1}} - \frac{\mathcal{W}_1(\alpha)}{2\alpha^2} \right] \zeta_*(k) + \frac{3}{8} R_\gamma \Omega_B(k) \left[\frac{\mathcal{W}_2(\alpha)}{\alpha^2} - \frac{2\alpha^2}{(3\alpha+4)\sqrt{\alpha+1}} \right] \right\}, \quad (3.7)$$

where

$$\begin{aligned} \mathcal{W}_1(\alpha) &= \frac{2}{15\sqrt{\alpha+1}} \{16[\sqrt{\alpha}-1] + \alpha[\alpha(9\alpha+2)-8]\}, \\ \mathcal{W}_2(\alpha) &= \frac{2}{5\sqrt{\alpha+1}} \{16[1-\sqrt{\alpha+1}] + \alpha[8+\alpha(\alpha-2)]\}. \end{aligned} \quad (3.8)$$

Thanks to the success of big-bang nucleosynthesis, it is rather plausible to imagine that the Universe was already dominated by radiation for temperatures as large and few MeV. However, prior to that time there are no direct probes of the expansion rate of the Universe. In a somehow indirect way this could be achieved through the study of the cosmic background of gravitational waves. At the moment, for instance, there is no compelling evidence of the fact that, after inflation, the Universe became suddenly dominated by radiation. It is, on the contrary, rather reasonable that, before settling on a radiation-dominated stage of expansion the Universe passed through a phase where, for instance, the rate of expansion was smaller than the Hubble rate during radiation. This occurrence is realized when the total barotropic index of the sources driving the geometry satisfies $1/3 < w_t \leq 1$. In this case the sources are said to be stiffer than radiation [47]. The stiffest equation of state we can imagine is the one where the barotropic index is 1 which implies that the sound speed coincides with the speed of light. The case of speed of sound equal to speed of light is the one contemplated by the so-called Zeldovich model (see [50] and references therein). A similar kind of evolution arises in quintessential inflationary models where the inflaton and the quintessence field are unified in a single degree of freedom. In this case (as in the more general case of stiffer phases [47]) the spectrum of relic gravitons presents a sharp increase [51] and a peak [52] which are potentially accessible to direct observations. In the context of quintessential inflation the stiff epoch is effectively dominated by the kinetic energy of the inflaton. Stiff phases also arise in brane-world scenarios [53] where the calculation of the graviton spectrum mirrors the four-dimensional case [51, 52].

The transition from a stiff epoch to a radiation-dominated phase of expansion can be understood in terms of the following exact solution:

$$\alpha = \frac{a}{a_r} = \sqrt{y^2 + 2y}, \quad y = \frac{\tau}{\tau_1}, \quad \tau_1 = \frac{2}{\lambda H_*}, \quad (3.9)$$

where

$$a_r = a_* \sqrt{\frac{\rho_{s*}}{\rho_{R*}}} \simeq \frac{M_P}{H_*}, \quad \lambda = a_* \frac{H_*}{M_P} \quad (3.10)$$

Equations (3.9) and (3.10) are solutions of Eqs. (2.1), (2.2) and (2.3) when the sources of the geometry are given in terms of a mixture of radiation and of a stiff fluid with $p_s = \rho_s$. Equations (3.9) and (3.10) parametrize the physical situation where, at τ_* some (small) amount of radiation is present in comparison with the stiff contribution (i.e. $\rho_{R*} \ll \rho_{s*}$). In the context of quintessential inflationary models

[54] the initial amount of radiation comes indeed from quantum fluctuations [55] and, consequently, $\rho_{R*} \simeq H_*^4$. This occurrence implies, in turn, that the hierarchy between the initial scale factor at τ_* and the scale factor at the onset of radiation (i.e. a_r is determined by M_P/H_*). Since $H_* < 10^{-6}M_P$, the duration of the stiff phase is correctly bounded because $H_r > H_{\text{bbn}}$. According to Eq. (2.4), the barotropic index and the sound speed are:

$$w_t = \frac{1}{3} \frac{\alpha^2 + 3}{\alpha^2 + 1}, \quad c_{\text{st}}^2 = \frac{2\alpha^2 + 9}{3(2\alpha^2 + 3)}. \quad (3.11)$$

Using therefore Eq. (3.11) inside Eq. (2.15) and changing variable from τ to α :

$$\frac{d\zeta}{d\alpha} = \frac{3R_\gamma\Omega_B\alpha}{(2\alpha^2 + 3)^2}. \quad (3.12)$$

Integrating Eq. (3.12) between $\alpha = 0$ and α_f we do get

$$\zeta(k, \tau) = \zeta_*(k) + \frac{R_\gamma\Omega_B(k)\alpha_f^2}{2(2\alpha_f^2 + 3)}, \quad (3.13)$$

where $\alpha_f \gg 1$ and it is defined deep in the radiation epoch. This result implies that the magnetic contribution enhances (rather than canceling) the adiabatic term $\zeta_*(k)$ of inflationary origin.

As in the case of the radiation-matter transition the total density contrast and the total peculiar velocity can be computed. In Fourier space the result is:

$$\epsilon_m(k, \tau) = -\frac{k^2\tau_*^2}{6\sqrt{\alpha^2 + 1}}[2\zeta_*(k)\mathcal{W}_3(\alpha) + R_\gamma\Omega_B(k)\mathcal{W}_4(\alpha)], \quad (3.14)$$

$$\begin{aligned} \theta_t(k, \tau) = & -k^2\tau_* \left\{ \left[\frac{\alpha^2}{\sqrt{\alpha^2 + 1}} - \frac{2\mathcal{W}_3(\alpha)}{\alpha^2} \right] \zeta_*(k) \right. \\ & \left. + \frac{R_\gamma\Omega_B(k)}{2} \left[\frac{\alpha^4}{(2\alpha^2 + 3)\sqrt{\alpha^2 + 1}} - \frac{2}{\alpha^2}\mathcal{W}_4(\alpha) \right] \right\}, \end{aligned} \quad (3.15)$$

where

$$\begin{aligned} \mathcal{W}_3(\alpha) &= \frac{4}{3}[(\alpha^2 + 1)^{3/2} - 1] - \frac{2\alpha^2}{\sqrt{\alpha^2 + 1}}, \\ \mathcal{W}_4(\alpha) &= \frac{2}{3}[(\alpha^2 + 1)^{3/2} + 8] - \frac{2(2\alpha^2 + 3)}{\sqrt{\alpha^2 + 1}}. \end{aligned} \quad (3.16)$$

This result can be generalized when the stiff phase is parametrized in terms of a source $p_s = \delta\rho_s$ with $1 < \delta < 1/3$. Repeating the same steps outlined above we will have that the dependence of the barotropic index and of the sound speed upon the scale factor are given, in this case, by:

$$w_t = \frac{1}{3} \left(\frac{3\delta + \alpha^{3\delta-1}}{1 + \alpha^{3\delta-1}} \right), \quad c_{\text{st}}^2 = \frac{9\delta(\delta + 1) + 4\alpha^{3\delta-1}}{3[3(\delta + 1) + 4\alpha^{3\delta-1}]}. \quad (3.17)$$

The equation for ζ and its related solution can be written as

$$\frac{d\zeta}{d\alpha} = 3R_\gamma\Omega_B \frac{(\delta + 1)(3\delta - 1)\alpha^{3\delta-2}}{[3(\delta + 1) + 4\alpha^{3\delta-1}]^2}, \quad (3.18)$$

$$\zeta(k, \tau) = \zeta_*(k) + R_\gamma\Omega_B(k) \frac{\alpha_f^{3\delta-1}}{4\alpha_f^{3\delta-1} + 3(\delta + 1)}. \quad (3.19)$$

As in the other two cases ϵ_m and θ_t can be easily computed:

$$\epsilon_m(k, \tau) = \frac{k^2 \tau_*^2}{9\delta^2 - 1} \frac{\alpha^{3(\delta-1)/2}}{\sqrt{1 + \alpha^{3\delta-1}}} [\mathcal{W}_5(\alpha, \delta) \zeta_*(\vec{k}) + R_\gamma \mathcal{W}_6(\alpha, \delta) \Omega_B(k)], \quad (3.20)$$

$$\theta_t(k, \tau) = \frac{k^2 \tau_*}{\sqrt{3\delta + 1}} \frac{\alpha^{(3\delta+1)/2}}{\sqrt{\alpha^{3\delta-1} + 1}} \left\{ \zeta_*(k) \left[1 - \frac{\sqrt{\alpha^{3\delta-1} + 1}}{2(3\delta - 1)} \frac{\mathcal{W}_5(\alpha, \delta)}{\alpha^{(3\delta+5)/2}} \right] \right. \\ \left. R_\gamma \Omega_B(\vec{k}) \left[\frac{\alpha^{3\delta-1}}{4\alpha^{3\delta-1} + 3(\delta + 1)} - \frac{\sqrt{\alpha^{3\delta-1} + 1}}{\alpha^{(3\delta+5)/2}} \frac{\mathcal{W}_6(\alpha, \delta)}{2(3\delta - 1)} \right] \right\}, \quad (3.21)$$

where

$$\mathcal{W}_5(\alpha, \delta) = \int_0^{s(\alpha)} \frac{4s + 3(\delta + 1)}{(s + 1)^{3/2}} s^{\frac{7-3\delta}{2(3\delta-1)}} ds, \\ \mathcal{W}_6(\alpha, \delta) = \int_0^{s(\alpha)} \frac{s^{\frac{5+3\delta}{2(3\delta-1)}}}{(s + 1)^{3/2}} ds. \quad (3.22)$$

The upper limit of integration in Eqs. (3.22) corresponds to $s(\alpha) = \alpha^{3\delta-1}$. For each value of δ the above integrals can be evaluated in explicit terms.

Suppose now to investigate a three stage model where the Universe expanded, initially, at a rate that was slower than radiation then got trapped in a radiation phase which turned subsequently into an epoch dominated by dusty matter. In this case we will have that the barotropic index and the sound speed are given, respectively, by:

$$w_t = \frac{1}{3} \frac{3 + \alpha^2}{1 + \alpha^2 + b\alpha^3}, \quad b = \frac{\rho_{M*}}{\rho_{S*}} \left(\frac{\rho_{S*}}{\rho_{R*}} \right)^{3/2}, \quad (3.23)$$

$$c_{st}^2 = \frac{18 + 4\alpha^2}{18 + 12\alpha^2 + 9b\alpha^3}. \quad (3.24)$$

In this case the evolution equation of curvature perturbations is given by

$$\frac{d\zeta}{d\alpha} = -3R_\gamma \Omega_B \frac{\alpha(\alpha^3 b - 4)}{(3\alpha^3 b + 4\alpha^2 + 6)^2}. \quad (3.25)$$

The (approximate) solution of Eq. (3.25) in the matter-dominated epoch reads:

$$\zeta(k, \tau) \simeq \zeta_*(k) + \frac{R_\gamma \Omega_B(k)}{3\alpha_{\text{rec}} + 4}. \quad (3.26)$$

The result of Eq. (3.26) shows an extra suppression of a factor $\alpha_{\text{rec}} \simeq 1/3$ in comparison with Eq. (3.5). This suppression can be easily understood. The evolution described by Eqs. (3.23) and (3.24) implies that, right after inflation, the Universe expands slower than radiation. When radiation kicks in, the curvature perturbations are enhanced. Later on, when dusty matter becomes dominant (around matter-radiation equality) the magnetized contribution tends, again, to cancel the pre-existing adiabatic mode. The net result of the initial increase and of the subsequent decrease of ζ is given in Eq. (3.26) and it is a bit different from the result of Eq. (3.5) where the intermediate stiff phase was absent. The following conclusions can then be drawn:

- if the Universe is dominated by radiation from the end of inflation (as it happens in the case of the standard evolution) the magnetized contribution and the adiabatic mode have opposite sign;

- if, prior to the electroweak epoch, the thermodynamic history of the Universe deviates from a radiation epoch the magnetized contribution is more suppressed in comparison with the standard case.

In the framework of conventional inflationary models this type of deviation from the standard scenario is pretty general. By general we mean that, within the current bounds on the expansion of the Universe arising from big-bang nucleosynthesis we can just imagine drastic deviation from the radiation-dominated evolution between the end of inflation and, say, neutrino decoupling. In fact, deviation from a radiation-dominated evolution after (or right before) big bang nucleosynthesis will necessarily jeopardize the production of the abundances of the light elements.

Up to now it has been assumed that the fluids of the primeval plasma do not exchange energy. Let us now address this interesting situation that could arise, for instance, in the course of reheating. Let us therefore imagine that a matter fluid (which can model the coherent oscillations of the inflaton) decays into massless particles. This dynamics can be parametrized by the following system ⁶:

$$\dot{H} = -4\pi G\left(\frac{4}{3}\rho_r + \rho_m\right), \quad (3.27)$$

$$\dot{\rho}_m = -3H\rho_m - \Gamma\rho_m, \quad (3.28)$$

$$\dot{\rho}_r = -4H\rho_r + \Gamma\rho_m. \quad (3.29)$$

The Universe, initially dominated (right after inflation) by dusty matter, becomes rapidly dominated by radiation at a rate that is controlled by $\bar{\Gamma}$. It should be immediately noticed that, by summing up Eqs. (3.28) and (3.29) the total energy density $\rho_t = \rho_r + \rho_m$ is covariantly conserved, i.e. $\dot{\rho}_t + 3H(\rho_t + p_t) = 0$. Equations (3.28) and (3.29) can be approximately solved:

$$\rho_m(t) = \rho_r(t_i)\left(\frac{a_i}{a}\right)^3 e^{-\bar{\Gamma}(t-t_i)}, \quad \rho_r(t) \simeq \rho_r(t_d)\left(\frac{a_d}{a}\right)^4, \quad (3.30)$$

where $t_d \simeq \bar{\Gamma}^{-1}$. As a consequence of the relations of Eq. (3.30) we can also say that

$$\frac{\rho_m}{\rho_r} \simeq \frac{H_1^2}{H_d^2}\left(\frac{a_i}{a}\right)^3 \left(\frac{a}{a_d}\right)^4 e^{-\bar{\Gamma}(t-t_i)} \simeq (t\bar{\Gamma})^{1/2} e^{-\bar{\Gamma}(t-t_i)} \quad (3.31)$$

In this situation the total barotropic index and the total sound speed are slightly modified thanks to the physical differences of the system. In particular we will have that

$$c_{\text{st}}^2 = \frac{4}{3} \frac{\rho_r}{4\rho_r + 3\rho_m} - \frac{\bar{\Gamma}}{3H} \frac{\rho_m}{4\rho_r + 3\rho_m}. \quad (3.32)$$

From Eq. (3.32) is clear that $c_{\text{st}}^2 \rightarrow 1/3$ when $\bar{\Gamma} \gg H$.

The evolution equations of curvature perturbations to be solved read:

$$\dot{\zeta} = -\frac{H}{p_t + \rho_t} \delta p_{\text{nad}} + \frac{H}{p_t + \rho_t} \left(c_{\text{st}}^2 - \frac{1}{3}\right) \delta \rho_B, \quad (3.33)$$

$$\dot{\zeta}_m = \frac{\dot{g}}{g} \zeta_m - \bar{\Gamma} g \frac{\dot{H}}{H^2} \zeta, \quad (3.34)$$

⁶Here we passed from the conformal to the cosmic time parametrization. See the comments after Eqs. (2.1), (2.2) and (2.3).

where $g = H/(\bar{\Gamma} + 3H)$. Let us now concentrate, as discussed above, on the conventional situation where the non-adiabatic modes are totally absent. In this case, initially, $\delta p_{\text{nad}} \propto (\zeta_r - \zeta_m) \simeq 0$ and $\zeta_r = \zeta_m \simeq \zeta_*$. Using Eq. (3.32) inside Eq. (3.33) we will simply have that

$$\dot{\zeta} = -\frac{H\delta\rho_B\rho_m}{g(4\rho_r + 3\rho_m)^2} \quad (3.35)$$

Recalling that, after t_d , $\bar{\Gamma} \gg H$ and ρ_m is exponentially suppressed, Eq. (3.35) can be written as

$$\frac{d\zeta}{dx} = -\frac{R_\gamma\Omega_B}{16}\sqrt{x}e^{-x}, \quad x = \bar{\Gamma}t. \quad (3.36)$$

Integrating once Eq. (3.36) the result will be

$$\zeta(k, y) = \zeta_*(k) - \frac{R_\gamma\Omega_B(k)}{16} \int_1^y \sqrt{x}e^{-x} dx. \quad (3.37)$$

The integral mentioned above can be done introducing the error function, i.e.

$$\int_1^y \sqrt{x}e^{-x} dx = \frac{1}{e} - \frac{\sqrt{y}}{e^y} - \frac{\sqrt{\pi}\text{Erf}(1)}{2} + \frac{\sqrt{\pi}\text{Erf}(\sqrt{y})}{2}. \quad (3.38)$$

Taking the limit $y \rightarrow \infty$, we then have

$$\zeta(k, t) \rightarrow \zeta_*(k) - \frac{R_\gamma\Omega_B(k)}{16} \left(\frac{2 + e\sqrt{\pi} - e\sqrt{\pi}\text{Erf}(1)}{2e} \right). \quad (3.39)$$

that is, numerically,

$$\zeta(k, t) \sim \zeta_*(k) - 0.079 R_\gamma\Omega_B(k) \sim \zeta_*(k) - \frac{R_\gamma\Omega_B(k)}{12}. \quad (3.40)$$

4 Bounds on different thermal histories

The two-point correlation function of curvature perturbations will receive contributions, in general, from the adiabatic mode, from one (or more) non-adiabatic modes, and from the magnetic field. As argued in the previous sections, the simplest situation is the one where only the adiabatic mode is present together with the magnetized contribution that we ought to constrain. This choice is motivated by the experimental evidence that the Doppler peak structure of the temperature autocorrelations strongly suggests that, after equality, the large-scale curvature perturbations were, predominantly adiabatic [22, 23, 24, 25, 26].

Consider therefore, the curvature perturbations present at recombination in the framework of the different thermal histories discussed in the previous section. The curvature perturbations can be written, in Fourier space, as ⁷

$$\zeta_h(k, \alpha_{\text{rec}}) = \zeta_*(k) + T_h(\alpha_{\text{rec}}, h_0^2\Omega_{M0})\Omega_B(k), \quad (4.1)$$

where the subscript h refers to each different thermal history and where $\zeta_*(k)$ represents the adiabatic contribution normalized to the large-scale value of the (ordinary) Sachs-Wolfe contribution to the

⁷The quantity $T_h(\alpha_{\text{rec}}, h_0^2\Omega_{M0})$ is the generalized transfer function that may change depending upon the specific thermal history labeled by the subscript h .

temperature autocorrelations. The total (scalar) power spectrum $\mathcal{P}_h(k)$, i.e. the Fourier transform of the two-point function computed at different spatial locations but at the same time is defined as

$$\langle \zeta_h(\tau, \vec{x}) \zeta_h(\tau, \vec{y}) \rangle = \int d \ln k \mathcal{P}_h(k) \frac{\sin kr}{kr}, \quad r = |\vec{x} - \vec{y}|. \quad (4.2)$$

From Eq. (4.1) and within the conventions summarized by Eq. (4.2) we then have that

$$\langle \zeta_h(\vec{k}, \tau) \zeta_h(\vec{p}, \tau) \rangle = \frac{2\pi^2}{k^2} \mathcal{P}_h(k) \delta^{(3)}(\vec{k} + \vec{p}) \quad (4.3)$$

where

$$\mathcal{P}_h(k) = \mathcal{P}_\zeta(k) + T_h^2(\alpha_{\text{rec}}, h_0^2 \Omega_{\text{M}0}) \mathcal{P}_\Omega(k) + 2T_h(\alpha_{\text{rec}}, h_0^2 \Omega_{\text{M}0}) \sqrt{\mathcal{P}_\zeta(k)} \sqrt{\mathcal{P}_\Omega(k)} \cos \gamma, \quad (4.4)$$

where γ is the correlation angle between the adiabatic mode and the magnetized contribution. In Eq. (4.4) \mathcal{P}_ζ is the power spectrum of the adiabatic contribution defined as

$$\mathcal{P}_\zeta = \mathcal{A}_\zeta \left(\frac{k}{k_p} \right)^{n_\zeta - 1}, \quad \mathcal{A}_\zeta = \frac{2 \times 10^4}{9T_{\text{cmb}}^2} A(k_p) = 2.95 \times 10^{-9} A(k_p). \quad (4.5)$$

In Eq. (4.5) n_ζ is the spectral index of the adiabatic mode and \mathcal{A}_ζ is the amplitude referred to the pivot scale k_p . Following the WMAP conventions the value of the pivot scale will be fixed as $k_p = 0.002 \text{ Mpc}^{-1}$. The numerical factor appearing in the expression of \mathcal{A}_ζ has been obtained by taking consistently $T_{\text{cmb}} = 2.725 \times 10^6$ (expressed in units of μK). In the absence of any other contributions the WMAP 3-year data imply⁸ $n_\zeta \simeq 0.947$ and $A(k_p) \simeq 0.815$ when combined with the remaining cosmological data sets, i.e. supernovae and large scale structure⁹. In Eq. (4.5) the magnetic part of the correlation function is expressed as [13, 14]

$$\mathcal{P}_\Omega(k) = \mathcal{F}(\epsilon) \bar{\Omega}_{\text{BL}}^2 \left(\frac{k}{k_L} \right)^{2\epsilon}, \quad \mathcal{F}(\epsilon) = \frac{4(6 - \epsilon)(2\pi)^{2\epsilon}}{\epsilon(3 - 2\epsilon)\Gamma^2(\epsilon/2)}, \quad (4.6)$$

where 2ϵ the spectral index of the magnetic energy density fluctuations and k_L is the magnetic pivot scale that will be defined in a moment. In Eq. (4.6) we have that

$$\bar{\Omega}_{\text{BL}} = \frac{B_L^2}{8\pi\rho_\gamma} = 7.56 \times 10^{-9} \left(\frac{B_L}{\text{nG}} \right)^2. \quad (4.7)$$

In Eq. (4.7) B_L is the value of the magnetic field smoothed, through a Gaussian window function, over a typical comoving length L which is related to the magnetic pivot scale as $L = 2\pi/k_L$. In what follows the fiducial value $k_L = \text{Mpc}^{-1}$ will be consistently adopted. It is relevant to appreciate that B_L represents the smoothed magnetic field red-shifted to the present epoch. This convention is a bit confusing but we will follow it since it is a common practice in the field. The source of the possible confusion is, in short, the following. The field B_L is the value of the magnetic field at recombination redshifted to the present epoch and assuming magnetic flux conservation which is well justified since the value of the conductivity is always rather large. However, B_L is *not* the present value of the magnetic field intensity observed in galaxies and galaxy clusters. The rationale for this

⁸In this analysis the values of the cosmological parameters will be fixed to the best fit values of the WMAP data combined with the other sets of cosmological observables. This choice is not crucial since the values of the cosmological parameters are purely illustrative. The essential features of the present analysis are unchanged if the best fit values of the WMAP data alone (or partially combined with the other data sets) are consistently assumed.

⁹The data [32] and [35, 36] are not included in the joined analysis.

statement is that during the gravitational collapse of protogalaxies the magnetic field intensity B_L will be amplified by compressional amplification and, probably, also by some dynamo action. Assuming just compressional amplification (which is the most certain aspect of the dynamics) the amplification factor may be of the order 10^4 or even 10^5 .

Notice that, from Eq. (4.6) the nearly scale-invariant limit is achieved for $\epsilon < 1$. Furthermore, as discussed elsewhere, the power spectrum of the magnetic energy density, being quartic in the field intensities, is computed in terms of the appropriate convolutions that have been evaluated, to get to Eq. (4.6), for $\epsilon < 1$. It should be borne in mind that, in the opposite case (i.e. $\epsilon > 1$) the magnetic energy density has a violet spectrum. This implies that, at very large length-scales the gravitational effect will be negligible and that, furthermore, the most significant bounds on the intensity of the magnetic field will come from comoving momenta close to the diffusion scale. Notice that the nearly scale-invariant spectrum is rather suggestive also because it would imply a nearly scale-invariant spectrum of large-scale magnetic fields from galaxies, to clusters, to super-clusters. This observation is, today, beyond our observational capabilities. However, by looking at recent determinations of magnetic fields in clusters and in some typical supercluster, it is indeed tempting to speculate that the resulting power spectrum of the magnetic energy density is nearly scale-invariant.

The correlation function of curvature perturbations enters directly the determination of the ordinary Sachs-Wolfe contribution which is the dominant source of temperature anisotropies at large angular scales. Let us require that the magnetized contribution is always much smaller than the adiabatic contribution. So, we will assume, in a rather conservative approach, that the magnetized contribution is always smaller (by a factor η) than the adiabatic contribution. The parameter η can be $\mathcal{O}(10^{-3})$, in a conservative approach. Following this strategy the magnetic field intensity can be bounded in each thermal history of the Universe. Consider, for instance, the plots appearing in Fig. (1) where, on the vertical axis, the base 10 logarithm of the smoothed magnetic field is reported in units of nG. In the plot at the left the three different lines correspond to the cases of the three different histories discussed in the previous sections. These three different histories will imply three different functions T_h with $h = 1, 2, 3$ and with, in general $T_1 \neq T_2 \neq T_3$. At late times the functions T_h can be approximated as

$$T_1(\alpha_{\text{rec}}, h_0^2 \Omega_{M0}) \simeq \frac{3R_\gamma}{4} \frac{\alpha_{\text{rec}}}{3\alpha_{\text{rec}} + 4}, \quad (4.8)$$

$$T_2(\alpha_{\text{rec}}, h_0^2 \Omega_{M0}) \simeq \frac{R_\gamma}{3\alpha_{\text{rec}} + 4}, \quad (4.9)$$

$$T_3(\alpha_{\text{rec}}, h_0^2 \Omega_{M0}) \simeq \frac{R_\gamma}{12} \left(\frac{12\alpha_{\text{rec}} + 4}{3\alpha_{\text{rec}} + 4} \right). \quad (4.10)$$

The function T_1 arises in the simplest case, i.e. when the Universe, after a phase of conventional inflation, passes from a radiation-dominated epoch to the matter stage. In T_1 the reheating is assumed to be a sudden process. The function T_2 describes the situation when there is an intermediate stiff phase expanding at a rate slower than radiation. Finally the function T_3 arises when there is a prolonged reheating and then the Universe is, subsequently, dominated by radiation and matter. In Fig. 1 (plot at the left) we illustrate the bounds as a function of the magnetic spectral index. The region below each of the curves implies that the contribution of the magnetic field to the two-point function is smaller than 10^{-3} .

The less restrictive case is, surprisingly enough, T_2 . The rationale for this occurrence can be simply understood in terms of the results reported in the previous section. In the transition from the stiff

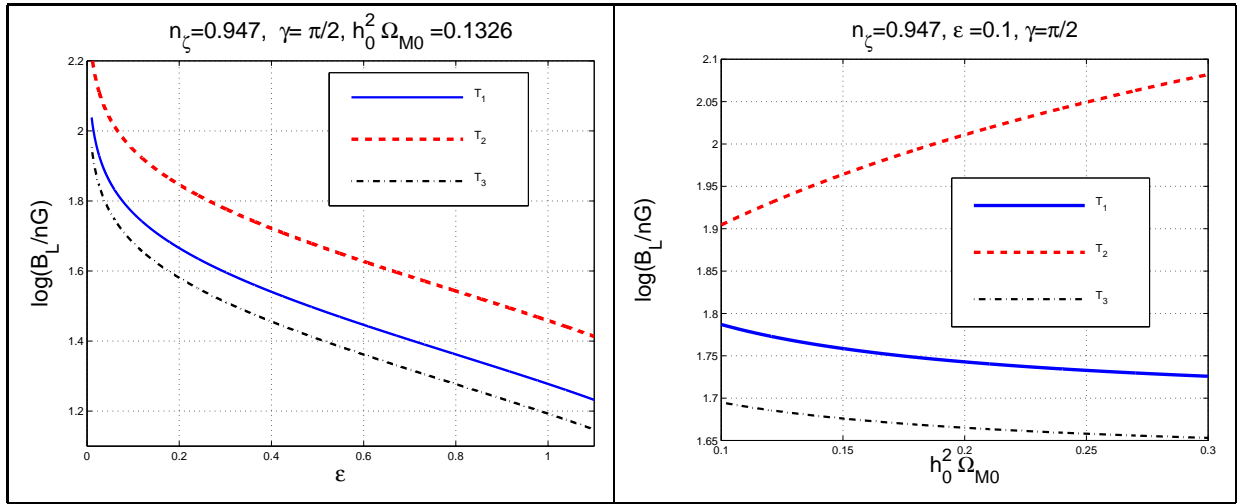


Figure 1: The bounds on the smoothed magnetic field intensity are illustrated as a function of the magnetic spectral index (plot at the left) and as a function of the critical fraction in dusty matter (plot at the right). The pivot scales k_p and k_L are fixed, respectively, to 0.002 Mpc^{-1} and Mpc^{-1} .

phase to the radiation phase the magnetized component gets reduced while in the subsequent transition from radiation to matter the magnetized contribution gets enhanced. Since the two effects tend to cancel, the net result will be an overall suppression of the magnetized contribution. This dynamical suppression allows the magnetic field amplitude to be larger than in the other two cases (i.e. T_1 and T_3) where there is no "destructive" interference between the two subsequent effects.

In the plot at the right of Fig. 1 this pattern is confirmed with an extra piece of information: if the matter fraction increases the bound become looser in the case of T_3 and a bit tighter in the case of T_1 and T_2 . In fact, in Fig. 1 (plot at the right) the magnetic spectral index has been kept fixed while the matter fraction is allowed to move from the fiducial value $h_0^2 \Omega_{M0} = 0.1326$ which is the one assumed in the left plot of Fig. 1. The increase (or decrease) of the critical fraction of dusty matter simply means, physically, that the recombination epoch is either delayed or anticipated.

It should also be remarked that the case of prolonged reheating is the most constraining. This occurrence can be also simply understood from the considerations of the previous section. In the case of prolonged reheating $c_{st}^2 \neq 1/3$. So during this phase the curvature perturbations decrease and this decrease will interfere constructively with the usual radiation matter transition since both contribution have the same sign. In Fig. 1 the value of the correlation angle has been fixed to $\pi/2$ implying that the adiabatic and the magnetized mode are uncorrelated. Again we may relax this assumption and allow γ to vary while all the other parameters are fixed to their fiducial values. This has been done in Fig. 2. As expected the bounds is tighter in the case when the two components are correlated and looser when the two components are anti-correlated. In Fig. 2 (plot at the right) the variation of the adiabatic spectral index is illustrated always in the case where the two components are uncorrelated. It is now relevant to remark that while $P_\zeta(k)$ slightly decreases as k increases, the opposite is true for $P_\Omega(k)$. It is therefore clear that, given this situation, the most constraining wavenumbers are the largest, i.e. the small-scale behaviour of the spectrum is the one that leads to the most stringent bounds. This consideration has been taken into account in deriving the bounds expressed by Figs. 1 and 2. In particular, it has been assumed that the diffusion scale is the one roughly associated with

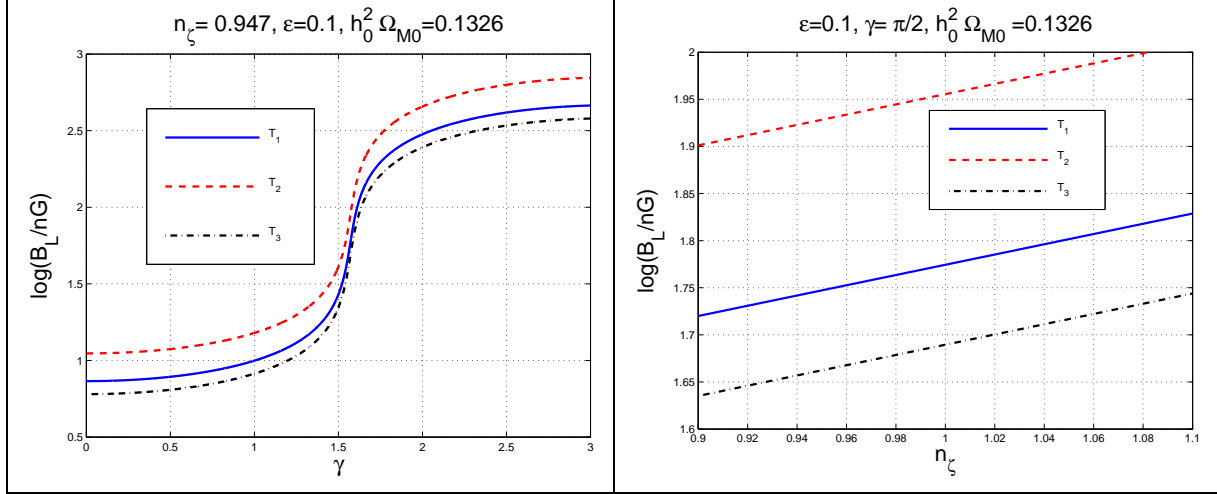


Figure 2: The bounds on the smoothed magnetic field intensity are illustrated as a function of the correlation angle γ (plot at the left) and as a function of the adiabatic spectral index n_ζ (plot at the right). All the other parameters are kept fixed to their fiducial values.

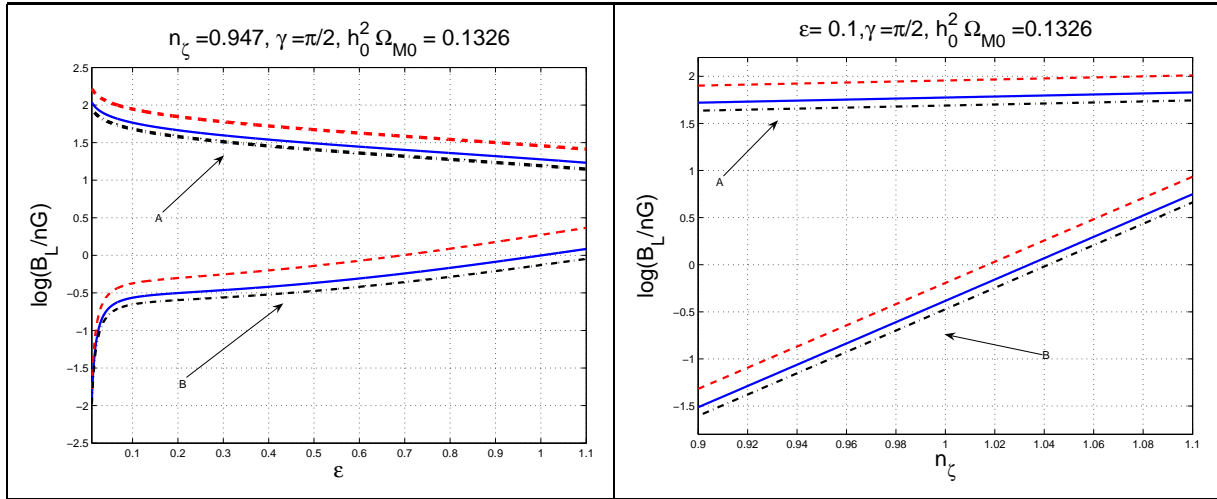


Figure 3: The potential differences in the estimate of the diffusion scale are illustrated. In the plot at the left, the bunch of curves labeled by B corresponds to the estimate of the diffusion scale given in Eq. (4.12) while the curves labeled by A are the same illustrated in Fig. 1 (plot at the left). In the plot at the right the two classes of curves have illustrate the same phenomenon but in terms of the dependence on n_ζ and should be compared with the right plot appearing in Fig. 2.

the Silk wavenumber, i.e.

$$\frac{1}{k_D \tau_{\text{rec}}} = 9.63 \times 10^{-3} \left(\frac{h_0^2 \Omega_b}{0.023} \right)^{-1/2} \left(\frac{h_0^2 \Omega_M}{0.134} \right)^{1/4} \left(\frac{1050}{z_{\text{rec}}} \right)^{3/4}. \quad (4.11)$$

There might be slightly different choices for the diffusion scale. For instance it has been noticed in the past that the diffusion scale of the magnetic fields should be related with the induced velocity of Alfvén waves. In this case the diffusion length-scale will be slightly smaller than the Silk scale by a factor which is essentially proportional, in our notations, to $(B_L/n\text{G})$. In this case the diffusion wavenumber will be given by [19]:

$$k_D \simeq (1.7 \times 10^2)^{2/\epsilon} \left(\frac{B_L}{n\text{G}} \right)^{-2/(\epsilon+2)} h_0^{1/(\epsilon+2)} \text{Mpc}^{-1} \quad (4.12)$$

Figure 3 illustrates the situation described by Eq. (4.12). It is clear that the patterns of the different thermal histories remain the same. However, the bound is improved by roughly one order of magnitude.

5 Concluding remarks

There are various lessons that can be drawn from the exercise reported in this paper. The main question we addressed has been the possible influence of slight variations in the thermal history of the Universe on the curvature perturbations induced by a magnetic field present for typical scales that are larger than the Hubble radius at recombination. Various inflationary mechanisms for the generation of cosmic magnetic field fall in this situation. It has been found that, indeed, the thermal history of the Universe may either suppress or increase the relative weight of magnetized curvature perturbations. The suppression occurs when, during the dynamical evolution, there is a sort of destructive interference. This phenomenon takes place, amusingly enough, when there was a phase, in the life of the Universe, when the rate of expansion was slower than the one of radiation. This kind of evolution must occur prior to the onset of big-bang nucleosynthesis and explicit examples have been provided. Also the opposite phenomenon can be realized, i.e. a sort of constructive interference when the overall contribution of the magnetized curvature perturbations gets enhanced in comparison with the adiabatic contribution present at the end of inflation. This situation takes place if the reheating phase is sufficiently prolonged in comparison with the sudden reheating approximation.

These considerations can certainly be developed along different directions. It is interesting to remark that the nature of the bounds on the magnetic field intensity may change quantitatively and qualitatively. Different thermal histories imply that the constraints on the magnetic field intensities may vary, generally speaking, of one order of magnitude. In the case when the Universe contains after inflation (but before radiation) a stiff phase the present value of the smoothed magnetic field must be qualitatively¹⁰ $B_L < 1.5 \times 10^{-7} \text{G}$ while in the context of prolonged reheating it must be as small as $1.6 \times 10^{-8} \text{G}$.

The presented considerations are not totally insensitive on the estimate of the diffusive wavenumber. In particular, it occurs that while experimental data favour a slightly red spectrum of curvature

¹⁰It should be stressed, as discussed in section 4, that B_L is the intensity of the magnetic field at recombination redshifted to the present epoch. This field is by no means equal to the present magnetic field. So the bounds on B_L are, really and truly, bounds on a primordial magnetized background. The present magnetic field of galaxies and clusters is certainly related to B_L . In the simplest case, compressional amplification may turn a 0.1 nG field (coherent over a comoving scale of the order of the Mpc) into the μG field observed in galaxies.

perturbations (i.e. an adiabatic spectral index slightly smaller than 1), the magnetized contribution is typically nearly scale-invariant but slightly blue. In this situation the most constraining wavenumbers are the ones close to diffusion scale. If the diffusivity length-scale is slightly smaller than the Silk scale, then the overall bounds on the smoothed magnetic field intensity range, depending on the details of the specific thermal history, from $B_L < \text{nG}$ to $B_L < 0.1 \text{ nG}$. It can be discussed if the Alfvén velocity should enter the thermal diffusivity scale when the magnetic field is fully inhomogeneous. Indeed Alfvén waves are only excited when there is a background magnetic field in the game. This is not the case when the magnetic field does not break spatial isotropy which the case investigated in the present paper and which is also, in our opinion, the most realistic one (see the introduction). With these caveats, however, it is important to notice that different thermal histories may either relax or improve the bounds on the magnetic field intensity by one order of magnitude.

References

- [1] Ya. B. Zeldovich, A. A. Ruzmaikin, and D.D. Sokoloff, *Magnetic Fields in Astrophysics* (Gordon and Breach Science, New York, 1983).
- [2] E. Battaner and E. Florido, *Fund. of Cosm. Phys.***21**, 1 (2000).
- [3] P. P. Kronberg, *Rep. Prog. Phys.***57**, 325 (1994).
- [4] M. Giovannini, *Int. J. Mod. Phys. D* **13**, 391 (2004)
- [5] B. Ratra, *Astrophys. J.* **391**, L1 (1992).
- [6] M. S. Turner and L. M. Widrow, *Phys. Rev. D* **37**, 2743 (1988).
- [7] M. Gasperini, M. Giovannini and G. Veneziano, *Phys. Rev. Lett.* **75**, 3796 (1995).
- [8] M. Giovannini, *Phys. Rev. D* **62**, 123505 (2000).
- [9] K. E. Kunze, *Phys. Lett. B* **623**, 1 (2005).
- [10] Ya. Zeldovich and I. Novikov, *The Structure and Evolution of the Universe*, (Chicago University Press, Chicago, 1971), Vol.2; Ya. Zeldovich, *Sov. Phys. JETP***21**, 656 (1965); K. Thorne, *Astrophys. J.* **148**, 51 (1967); S. Hawking and R. J. Tayler, *Nature* **309**, 1278 (1966); J. Barrow, *Mon. Not. R. Astron. Soc.* **175**, 359 (1976); J. Barrow, *Phys. Rev. D* **55**, 7451 (1997).
- [11] A. Hajian and T. Souradeep, *Phys. Rev. D* **74**, 123521 (2006); T. Souradeep, A. Hajian and S. Basak, *New Astron. Rev.* **50**, 889 (2006); P. D. Naselsky, L. Y. Chiang, P. Olesen and O. V. Verkhodanov, *Astrophys. J.* **615**, 45 (2004); G. Chen, P. Mukherjee, T. Kahniashvili, B. Ratra and Y. Wang, *Astrophys. J.* **611**, 655 (2004).
- [12] M. Giovannini, *Phys. Rev. D* **73**, 101302 (2006).
- [13] M. Giovannini, *Phys. Rev. D* **74**, 063002 (2006).
- [14] M. Giovannini, CERN-PH-TH/2007-110, arXiv:0706.4428 [astro-ph].
- [15] J. D. Barrow, R. Maartens and C. G. Tsagas, arXiv:astro-ph/0611537.
- [16] T. Kahniashvili and B. Ratra, *Phys. Rev. D* **75**, 023002 (2007).
- [17] K. Subramanian and J. D. Barrow, *Mon. Not. Roy. Astron. Soc.* **335**, L57 (2002).
- [18] K. Subramanian, T. R. Seshadri and J. D. Barrow, *Mon. Not. Roy. Astron. Soc.* **344**, L31 (2003).
- [19] A. Mack, T. Kahniashvili and A. Kosowsky, *Phys. Rev. D* **65**, 123004 (2002)
- [20] K. Subramanian, arXiv:astro-ph/0601570.
- [21] M. Giovannini, *Class. Quant. Grav.* **23**, R1 (2006).
- [22] D. N. Spergel *et al.* [WMAP Collaboration], arXiv:astro-ph/0603449.
- [23] L. Page *et al.* [WMAP Collaboration], arXiv:astro-ph/0603450.

- [24] H. V. Peiris *et al.* [WMAP Collaboration], *Astrophys. J. Suppl.* **148**, 213 (2003).
- [25] D. N. Spergel *et al.* [WMAP Collaboration], *Astrophys. J. Suppl.* **148**, 175 (2003).
- [26] C. L. Bennett *et al.* [WMAP Collaboration], *Astrophys. J. Suppl.* **148**, 1 (2003).
- [27] S. Cole *et al.* [The 2dFGRS Collaboration], *Mon. Not. Roy. Astron. Soc.* **362**, 505 (2005).
- [28] T. E. Montroy *et al.*, *Astrophys. J.* **647**, 813 (2006).
- [29] C. I. Kuo *et al.* [ACBAR collaboration], *Astrophys. J.* **600**, 32 (2004).
- [30] A. C. S. Readhead *et al.*, *Astrophys. J.* **609**, 498 (2004).
- [31] C. Dickinson *et al.*, *Mon. Not. Roy. Astron. Soc.* **353**, 732 (2004).
- [32] W. L. Freedman *et al.*, *Astrophys. J.* **553**, 47 (2001).
- [33] D. J. Eisenstein *et al.* [SDSS Collaboration], *Astrophys. J.* **633**, 560 (2005).
- [34] M. Tegmark *et al.* [SDSS Collaboration], *Astrophys. J.* **606**, 702 (2004).
- [35] E. Semboloni *et al.*, arXiv:astro-ph/0511090.
- [36] H. Hoekstra *et al.*, *Astrophys. J.* **647**, 116 (2006).
- [37] P. Astier *et al.* [The SNLS Collaboration], *Astron. Astrophys.* **447**, 31 (2006).
- [38] A. G. Riess *et al.* [Supernova Search Team Collaboration], *Astrophys. J.* **607**, 665 (2004).
- [39] B. J. Barris *et al.*, *Astrophys. J.* **602**, 571 (2004).
- [40] J. M. Bardeen, *Phys. Rev. D* **22**, 1882 (1980).
- [41] J. Bardeen, P. Steinhardt, M. Turner, *Phys. Rev. D* **28**, 679 (1983).
- [42] R. Brandenberger, R. Kahn, and W. Press, *Phys. Rev. D* **28**, 1809 (1983).
- [43] D. H. Lyth, *Phys. Rev. D* **31**, 1792 (1985).
- [44] W. Hu and N. Sugiyama, *Astrophys. J.* **444**, 489 (1995).
- [45] W. Hu and N. Sugiyama, *Astrophys. J.* **471**, 542 (1996).
- [46] H. Kodama and M. Sasaki, *Prog. Theor. Phys. Suppl.* **78**, 1 (1984).
- [47] M. Giovannini, *Phys. Rev. D* **58**, 083504 (1998).
- [48] V. Sahni, *Class. Quant. Grav.* **5**, L113 (1988).
- [49] V. Sahni, *Phys. Rev. D* **42**, 453 (1990).
- [50] L. P. Grishchuk, *Ann. N. Y. Acad. Sci.* **302**, 439 (1977).
- [51] M. Giovannini, *Phys. Rev. D* **60**, 123511 (1999).

- [52] M. Giovannini, *Class. Quant. Grav.* **16**, 2905 (1999).
- [53] V. Sahni, M. Sami and T. Souradeep, *Phys. Rev. D* **65**, 023518 (2002).
- [54] P. J. E. Peebles and A. Vilenkin, *Phys. Rev. D* **59**, 063505 (1999).
- [55] L. H. Ford, *Phys. Rev. D* **35**, 2955 (1987).